XV International Conference on Computational Plasticity. Fundamentals and Applications
COMPLAS 2019
E. Oñate, D.R.J. Owen, D. Peric , M. Chiumenti, and Eduardo de Souza Neto (Eds)

NEW DUCTILE FRACTURE CRITERION FOR PREDICTION OF INTERNAL FRACTURE IN SKEW ROLLING

KOJI YAMANE*, KAZUHIRO SHIMODA* AND KOICHI KURODA*

* Research and Development, Process Research Laboratories
Nippon Steel Corporation
1-8 Fuso-Cho, Amagasaki, Hyogo, 660-0891, Japan
e-mail: yamane.6nq.kohji@jp.nipponsteel.com

Key words: Skew Rolling, Internal fracture, Stress Triaxiality, Ductile Fracture Criterion.

Abstract. Skew rolling is the process of reducing the diameter of a round billet. In this process, internal fracture may occur in the rolled material. This phenomenon is known as the Mannesmann effect. While there has been great discussion about the mechanism of internal fracture, it has yet to be fully clarified. To investigate the internal fracture initiation and propagation, we conducted hot rolling experiments and evaluated the stress and strain of the rolled material by elasto-plastic finite element analysis. The results show that the internal fracture arises on the internal surface in which shear stress acts owing to the combined effect of tensile and shear stress. In this paper, a new ductile fracture criterion is discussed to quantitatively predict the occurrence of internal fracture in skew rolling.

1 INTRODUCTION

The skew rolling process is one method for reducing the diameter of a round billet [1]. In this process, a heated round billet is rotated and advanced by rolls as the roll axes are skewed counterclockwise to the pass line. Depending on the rolling conditions, internal fracture may occur in the rolled material. This phenomenon also occurs in cross rolling to form axially symmetric parts. The mechanism of internal fracture has been researched since the 20th century. On the basis of such studies, many researchers have proposed various theories on its mechanism: shear fracture theory [2–11], ductile fracture theory [12, 13], fatigue fracture theory [14] and so forth. However, since the theories are based on qualitative experimental results that have not been quantitatively evaluated, the mechanism of internal fracture has not been fully clarified. Therefore, this paper discusses the mechanism of internal fracture in three-roll skew rolling which has been little investigated. To investigate the internal fracture initiation and propagation, we conducted hot rolling experiments and quantitatively evaluated the stress and strain history of the rolled material by elasto-plastic finite element analysis. As a result, it was clarified that the internal fracture initiation points in skew rolling lay on a position away from the central axis parts of the rolled material where conventional ductile fracture criteria predicted maximum damage values. Because it is necessary to develop a reasonable model to describe internal fracture, this paper focuses on the validation of a new ductile fracture criterion to quantitatively predict the occurrence of internal fracture in skew rolling.

2 HOT ROLLING EXPERIMENTS

2.1 ROLLING CONDITIONS

In this paper, the actual situations of internal fracture in three-roll skew rolling were investigated. Figure 1 shows a schematic diagram of the three-roll skew rolling mill. This rolling mill is arranged with the rolls placed at circumferential intervals of 120° around the billet, and the roll axes are skewed to the pass line. This angle is referred to as feed angle β. The roll axes being skewed reduce the outer diameter of a material as it performs helix rotation. To investigate the internal fracture behavior in skew rolling, semi-finished products were cut with wire saws into multiple cross sections in the longitudinal direction. The rolling condition is shown in Table 1. The rolls rotate in the same direction with a constant rotational velocity of 100 rpm. The internal fracture was investigated by rolling the material at a feed angle β of 4°, with a billet diameter of 70 mm, a rolled diameter of 42 mm, and a material heating temperature of 1100°C. The chemical composition of the specimens is shown in Table 2. Free-cutting steel SUM24L with low deformability containing inclusions such as MnS and Pb was used for the specimens.

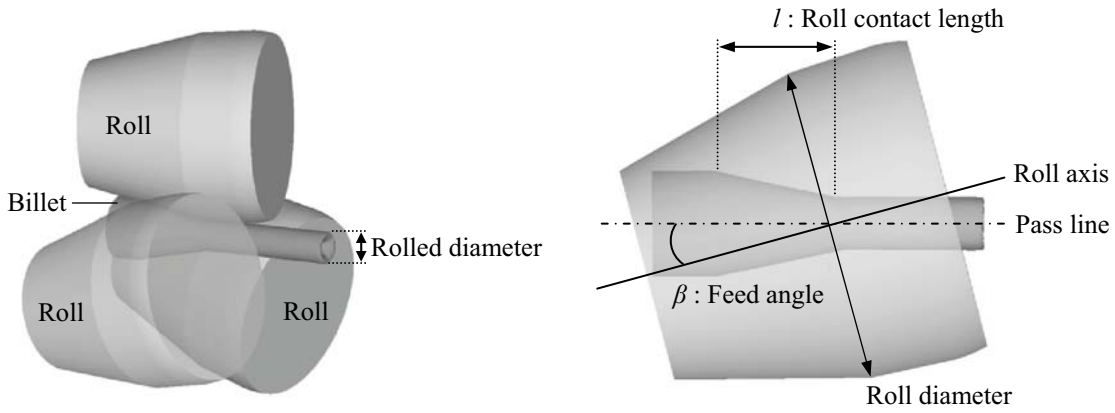

Figure 1: Schematic of skew rolling mill with three rolls

Table 1: Rolling conditions

Roll diameter [mm]	180
Billet diameter [mm]	70
Rolled diameter [mm]	42
Feed angle β [°]	4
Billet heating temperature [°C]	1100

Table 2: Chemical composition of SUM24L [wt.%]

C	Si	Mn	P	S	Pb	Fe
0.07	-	1.04	0.07	0.33	0.17	Bal.

2.2 OBSERVATION OF INTERNAL FRACTURE

A digital microscope VHX-6000 made by KEYENCE was used for the observation of internal fracture in the rolling cross section. The observation procedure is as follows:

(1) Create the entire image of a rolling cross section with high resolution, synthesizing the multiple-shot images of the rolling cross section at each position with magnification of 50, into a sheet of those images.

(2) Count black dots of more than 200 μm^2 (an average diameter of 16 μm) as one void after subjecting those images to binarization processing. Note that the resolution can be considered as adequate because 12 pixels constitute a void of 200 μm^2 as one side of a pixel has a length of 4.15 μm.

(3) Calculate the void density, i.e., the number of voids per unit area, by counting the number of voids at the each ring shaped area with 1 mm band breadth from the central axis of the rolled material as shown in Fig. 2.

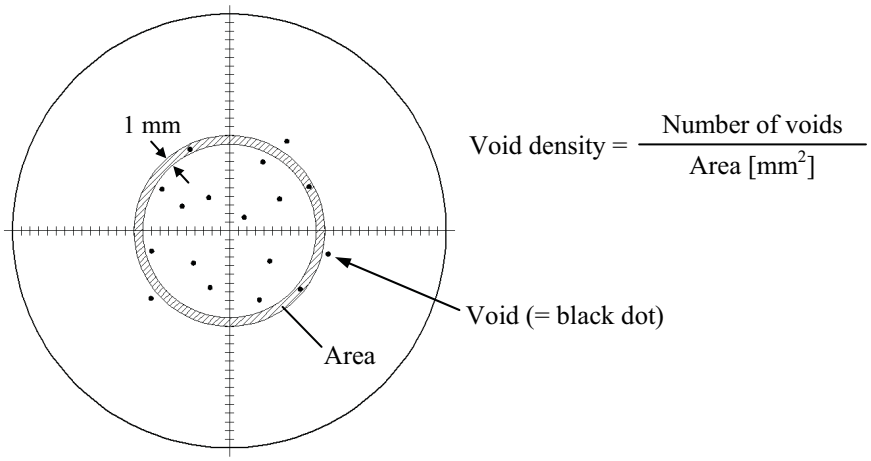

Figure 2: Measurement of void density in rolling cross section

2.3 EXPERIMENTAL RESULTS

Internal fracture was observed in the roll condition of feed angle $\beta = 4°$. Figure 3 shows the measurement position of a semi-finished product. The rolling cross sections each lying at -10 mm and +10 mm distance from termination point O of the outer diameter forming via the tapered roll faces were observed in detail. The macro photographs of the rolling cross section at feed angle $\beta = 4°$ are shown in Fig. 4. It was identified that voids nucleate at the location a couple of millimeters away from the central axis of the rolled materials, grow, and coalesce to each other in the circumferential direction, as the rolled materials advances, and thus, finally occur internal fracture. Figure 5 indicates the distribution of void density in the rolling cross section before the voids coalesce. Most of the voids at the initial stage of internal fracture had a diameter of 30 μm or less. The void density at the central axis of the rolled materials was 0 [/mm^2] in the rolling cross section A, and became high around a radius of 6 mm from the central axis. The fracture initiation points in three-roll skew rolling lay not in the central axis parts of the materials but in their surroundings.

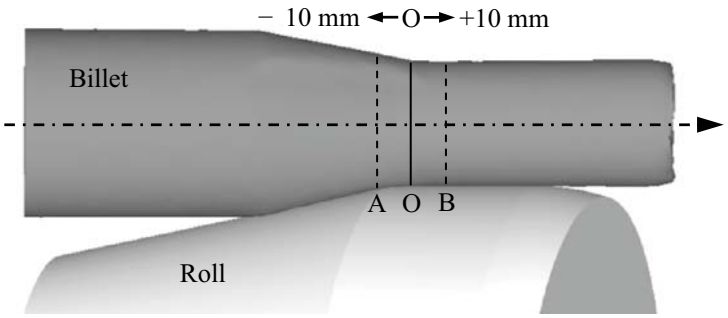

Figure 3: Measurement position of semi-finished product

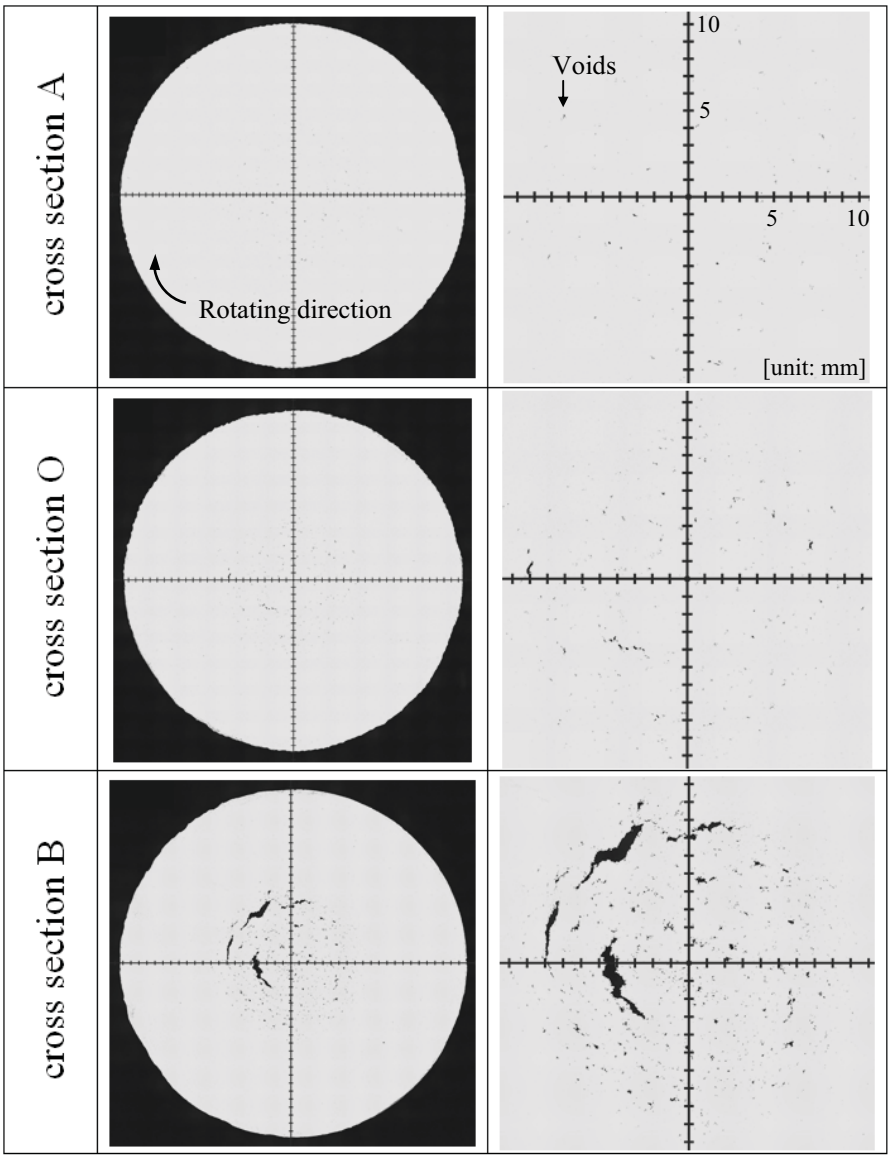

Figure 4: Photographs of voids in rolling cross sections

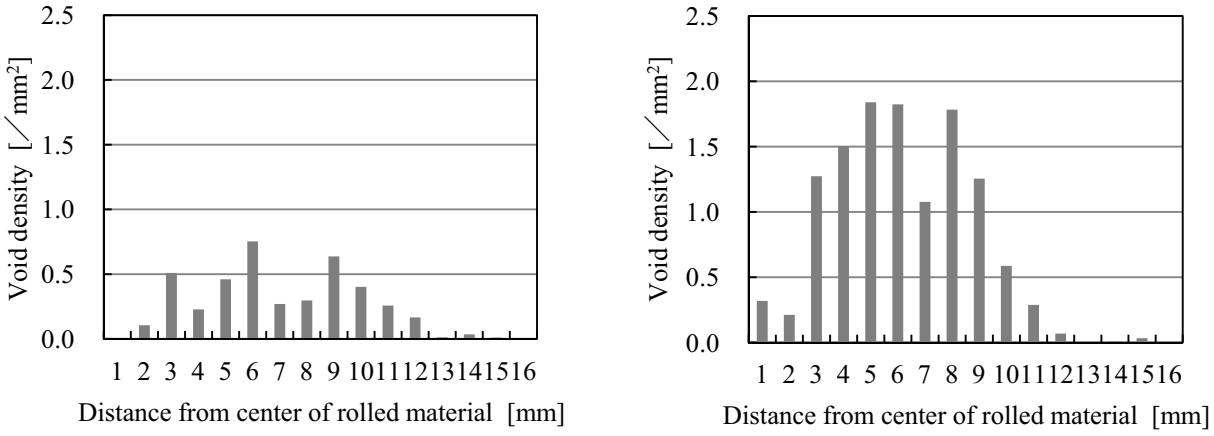

(a) Cross section A

(b) Cross section O

Figure 5: Distribution of void density in rolling cross sections

3 NUMERICAL ANALYSIS

3.1 NUMERICAL ANALYSIS MODEL

In order to investigate the deformation behavior inside the rolled material in skew rolling, three-dimensional deformation analysis was performed by the elasto-plastic finite element method using FE code Simufact Forming. The numerical analysis model was similar to the skew rolling mill as shown in Fig. 1; the rolls were modeled as rigid bodies, and a rolled material was modeled as hexahedral elements. The Coulomb friction coefficient of the roll was 0.5 because the contact condition between the material and rolls was assumed to be almost sticking. The material temperature, roll temperature, and heat transfer coefficient h between the material and rolls were, respectively, set to be 1100°C, invariable 20°C, and 4000 [W/m^2/K]. For the stress-strain curve of the rolled material, the hot tensile test results of the free-cutting steel SUM24L was selected among the MatILDa functions implemented in Simufact Forming. The selected function is shown in Formula (1). The equivalent stress σ_{eq} in the plastic deformation area is a function of the equivalent strain ε_{eq}, equivalent strain rate $\dot{\varepsilon}_{eq}$, and temperature T. The roll conditions for the numerical analysis were the same as those for the hot rolling experiments as shown in Table 1. The predictability of internal fracture was evaluated by comparing the experimental results with the damage value of ductile fracture criteria calculated by the numerical analyses. The damage accumuration is usually formulated with a function of stress and strain.

$$\sigma_{eq} = 1600 \cdot \exp(-0.00235 \cdot T) \cdot \varepsilon_{eq}^{\left(10^{-4} \cdot T - 0.04488\right)} \cdot \exp\left(\frac{-6.44 \cdot 10^{-6} \cdot T - 0.02466}{\varepsilon_{eq}}\right) \cdot \dot{\varepsilon}_{eq}^{\left(6.0 \cdot 10^{-5} \cdot T + 0.049492\right)} \quad (1)$$

3.2 CONVENTIONAL DUCTILE FRACTURE CRITERIA

Concerning the prediction of fracture in plastic processing, a variety of ductile fracture criteria are proposed by Ayada et al. [15], Oyane [16], Cockcroft & Latham [17], Rice & Tracey [18], McClintock [19], and Brozzo et al. [20]. The damage values in the experiments described in the previous chapter were calculated using the respective criteria; however, no criterion agreed with the distribution of the actual fracture. As an example, the damage values in the criterion by Ayada, which means the integral values of stress triaxiality σ_m/σ_{eq} ($\sigma_m = (\sigma_r+\sigma_\theta+\sigma_z)/3$) and the equivalent strain ε_{eq}, are shown in Fig. 6. The darker the contour, the higher the value, which means that fracture is more likely to occur. In three-roll skew rolling, high tensile stress works along the longitudinal direction in the central axis of the rolled material, and the stress triaxiality indicates the maximum value in the central axis parts. The compressive stresses in the radial direction are high in the vicinity of the portion in contact with the rolls, and the stress triaxiality indicates a negative value with a high absolute value. For the equivalent strain, the maximum is provided on the external surface of the materials due to the shear deformation with the rotation of the material. As a result, for the damage value, the maximum is provided in the central axis where the stress triaxiality always takes a positive value. Ayada's criterion is applied to the prediction of internal fracture during extrusion processing, and its efficacy is recognized; however, it can not be applied to predict internal fracture in skew rolling. This criterion assumes that the direction of the principal stress is constant, which may cause disagreement with the experimental results. The skew rolling mill is characterized by repeated sequential rolling, and the positive and negative values of the stress triaxiality alternate quite often with the rotation of the material so that the damage value fluctuates. Therefore, under the processing involving rotating materials, a new criterion that is represented by stress components coinciding with the fracture growth direction is needed for precise prediction of internal fracture.

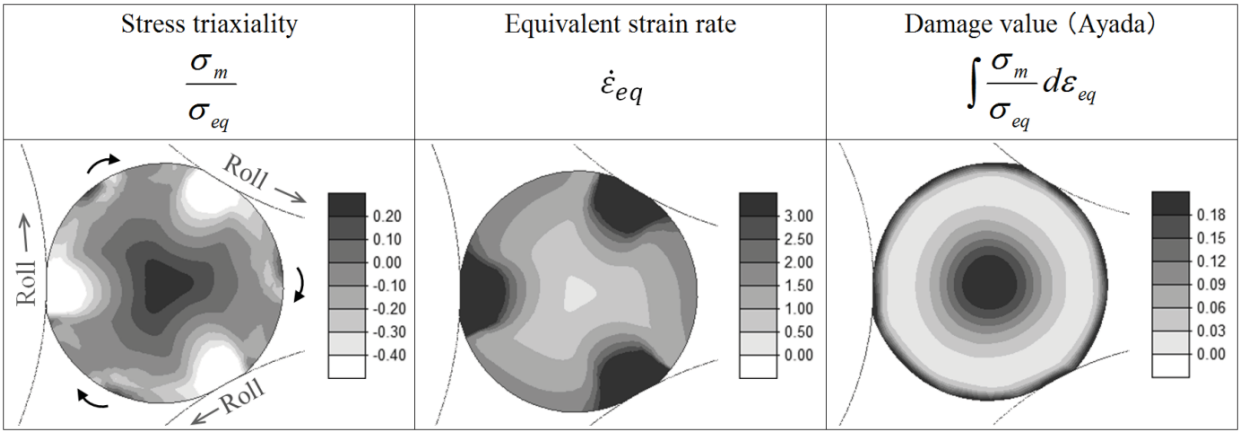

Figure 6: Distribution of damage value in criterion by Ayada

4 RESULTS AND DISCUSSION

4.1 EACH STRESS COMPONENT DURING ROLLING

Stress components inside the materials in three-roll skew rolling were specifically investigated. Figure 7 shows the six components of the stresses during rolling. Stress in the radial direction σ_r takes a compressive value of -80 MPa immediately under the rolls and a tensile value across the roll to roll. Circumferential stresses σ_θ provide a stress distribution opposite to that of σ_r. The materials meet the maximum stress triaxiality in the central axis parts, as stress in the longitudinal direction σ_z assumes significant tension in those parts. Shear stress in the circumferential direction $\sigma_{r\theta}$ works in the same manner as the principal stress. One of the characteristics of skew rolling is that tensile stress and shear stress work simultaneously, because the outer diameter is reduced while allowing the materials to rotate.

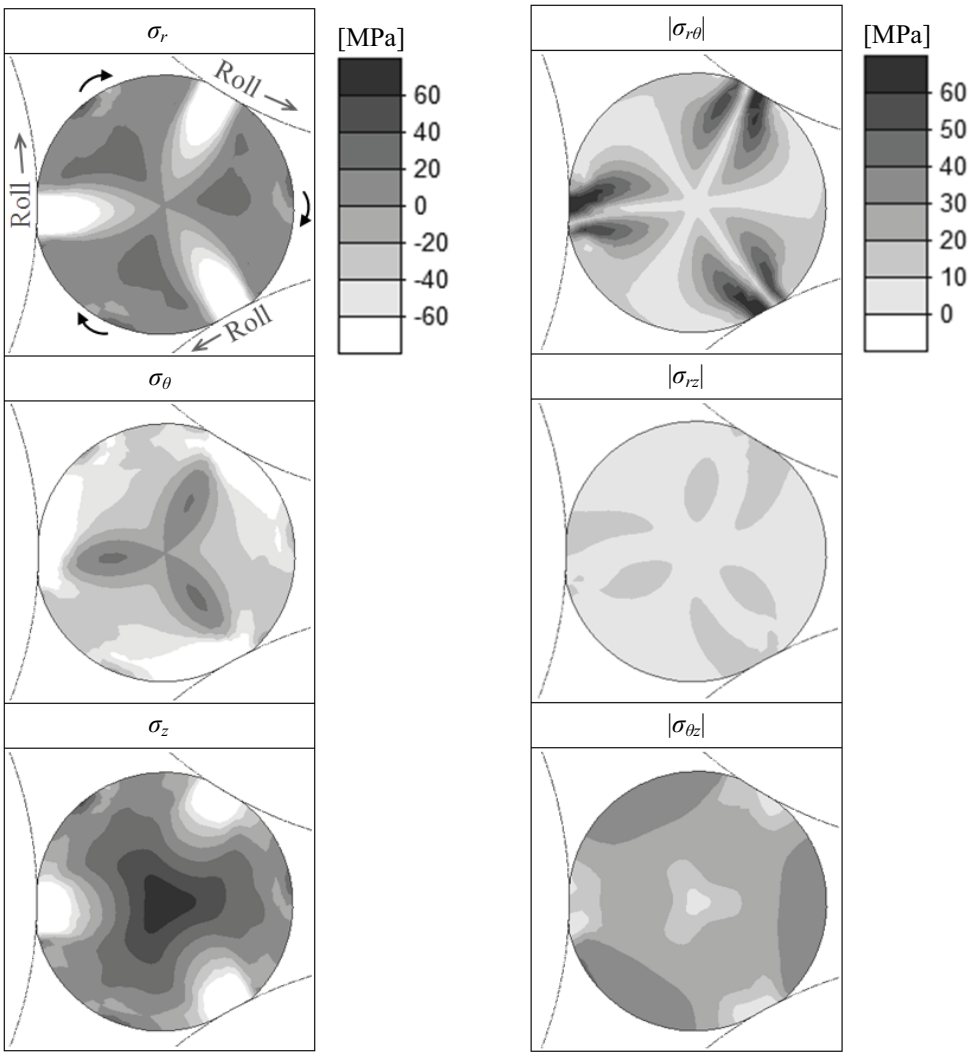

Figure 7: Distribution of stress in rolling cross section A

4.2 PROPOSAL OF NEW DUCTILE FRACTURE CRITERION

The conventional ductile fracture criteria do not agree with the experimental results because the effects of shear stress on void coalescence are not adequately estimated. For example, it is reported by Bao et al. [21–23], Weck et al. [24], Li et al. [25] and Lou et al. [26, 27] that shear stress can contribute to ductile fracture. Bao et al. stated that the value of the equivalent strain to fracture as well as the fracture form depend on the stress state. When the relationship between the stress triaxiality and the equivalent strain to fracture is further clarified, it can be seen that a void can grow and mainly cause ductile fracture if the stress triaxiality takes a positive value, i.e., the stress state is under tension. On the other hand, a void is unlikely to grow and shear fracture can occur if the stress triaxiality takes a negative value, i.e., the stress state is under compression. Furthermore, if the stress triaxiality takes a positive value with a low absolute value, it is proposed that void growth due to tensile stress, mixed with void coalescence due to shear stress, can lead to fracture. Weck et al. revealed the mechanism of void coalescence through performing tensile tests of alminium alloy sheets that have various laser drilled holes. When these specimens are pulled under the condition whereby artificial holes are arrayed, the holes coalesce to each other at 45° with respect to the tensile direction by shear deformation. Li et al. stated that the equivalent strain nucleates fine voids originating from inclusions, tensile stress promotes the growth of these voids, and shear stress allows the voids to coalesce with each other. Lou et al. stated that ductile fracture occurs via the processes of i) void nucleation, ii) void growth, and iii) void coalescence, analyzing the ductile fracture microscopically. They propose such functions as i) equivalent strain ε_{eq}, ii) stress triaxiality σ_m/σ_{eq}, and iii) maximum shear stress τ_{max} are appropriate when those respective phenomena are formulated.

Considering the above mentioned references and our reseach results that the internal fracture initiation shown in Fig. 4 correspond with the positions at which the tensile stress and the shear stress work simultaneously as shown in Fig. 7, we assumed that internal fracture occurs due to the synergistic effects of tensile and shear stress. It is postulated that the void nucleation, void growth, and void coalescence, respectively, are represented by equivalent strain ε_{eq}, tensile stress, and shear stress; these three factors are considered to be requirements for internal fracture. This paper presents a new ductile fracture criterion in which internal fracture is represented by a product of tensile stresses σ_r, σ_θ, and σ_z as well as shear stresses $\sigma_{r\theta}$, σ_{rz}, and $\sigma_{\theta z}$, and the equivalent strain ε_{eq}, concerning the plastic processing by which tensile stress works in phase with shear stress.

Figures 8 and 9, respectively, show a schematic diagram of the stress components, and a combination of normal stress components and shear stress components. The proposed criterion is composed of a combination of stresses that cause a single void to grow in the fracture growth direction observed from the rolling cross section. Therefore, the term of $\sigma_{\theta z}$ is excluded from the proposed criterion, as shear stress $\sigma_{\theta z}$ is assumed to have no impact on initiating internal fracture, because shear stress $\sigma_{\theta z}$ working in the helix direction of the rolled material is orthogonal to the fracture growth direction observed from the rolling cross section. $\sigma_r \cdot \sigma_{rz}$ is excluded from the proposed criterion to avoid duplex addition of the radial direction stress σ_r. Term σ_r has two types, i.e., $\sigma_r \cdot \sigma_{r\theta}$ and $\sigma_r \cdot \sigma_{rz}$, and is the combination of shear stress $\sigma_{r\theta}$ or σ_{rz} caused by the diameter reduction. As shown in Fig. 7, the distribution of stress $\sigma_{r\theta}$ agrees with that of σ_{rz} in the rolled material; $\sigma_{r\theta}$ has evidently large absolute values. That

makes the grown voids to coalesce along the direction in which $\sigma_{r\theta}$ works. The proposed criterion is constituted by such a combination of the three terms $\sigma_r \cdot \sigma_{r\theta}$, $\sigma_\theta \cdot \sigma_{r\theta}$, and $\sigma_z \cdot \sigma_{rz}$, which are assumed to significantly contribute to initiating internal fracture observed from the rolling cross section.

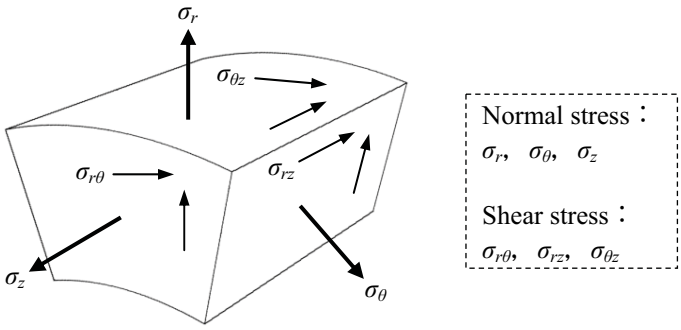

Figure 8: Schematic of each stress component

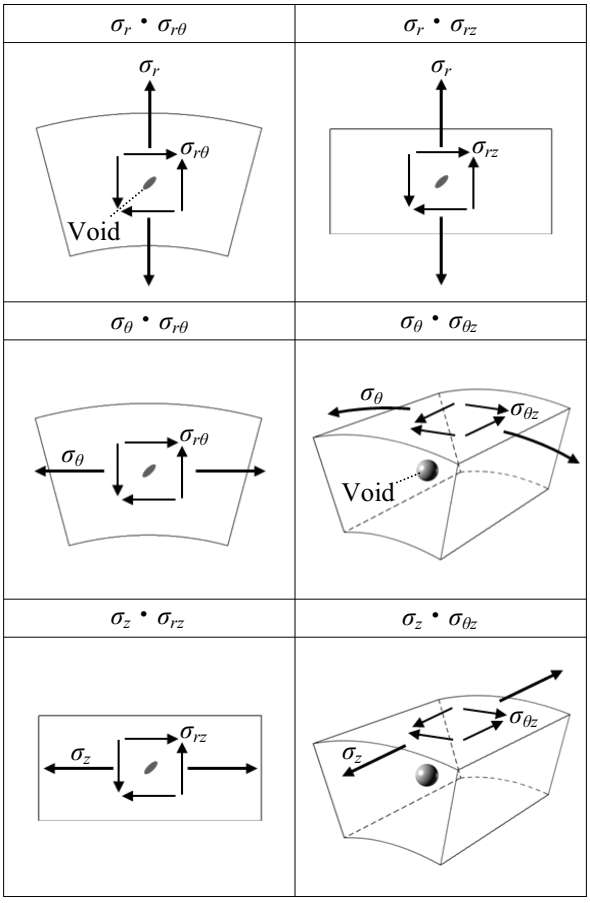

Figure 9: Schematic of combination of normal stress and shear stress

The proposed criterion is shown in Formulas (2) and (3). Shear stresses $\sigma_{r\theta}$ and σ_{rz} can take a negative value within the numerical analysis as their direction is reversed when the material rotates; The shear stress term is defined as an absolute value because shear stress contributes to fracture irrespective of taking a positive or negative value. The incremental value of damage per unit time f is a product of the dimensionless stress term and the equivalent strain rate $\dot{\varepsilon}_{eq}$. The damage value F is the incremental value f integrated with rolling time t, i.e., a product of the dimensionless stress term and the equivalent strain ε_{eq}. When the incremental value f turns positive, f is added as voids can nucleate and grow in a tensile stress field. In contrast, in a compressive stress field in which the increment value f turns negative, $f = 0$ is defined, considering that no voids ever grow, or that any nucleated voids neither shrink nor vanish.

$$f = \left\{ \left(\frac{\sigma_r}{\sigma_{eq}} \right) \left(\frac{|\sigma_{r\theta}|}{\sigma_{eq}} \right) + \left(\frac{\sigma_\theta}{\sigma_{eq}} \right) \left(\frac{|\sigma_{r\theta}|}{\sigma_{eq}} \right) + \left(\frac{\sigma_z}{\sigma_{eq}} \right) \left(\frac{|\sigma_{rz}|}{\sigma_{eq}} \right) \right\} \dot{\varepsilon}_{eq} \tag{2}$$

$$F = \int \langle f \rangle dt \qquad \langle f \rangle = \begin{cases} f & \text{when } f > 0 \\ 0 & \text{when } f \le 0 \end{cases} \tag{3}$$

Figure 10 shows the distribution of the incremental value of damage per unit time f and that of damage value F in the rolling cross section A. Damage value F was calculated from the user subroutines built into the FE code, or calculated by extracting the stress and strain histories from arbitrary integral points. Damage value F takes the maximum value at a position 6 mm away from the central axis parts of the rolled materials. This is because a position away from the central axis parts constitutes a stress field in which tensile stress and shear stress work simultaneously. The increment value f is low, since shear stresses $\sigma_{r\theta}$ and σ_{rz} can hardly work in the central axis parts. Furthermore, the increment value f becomes close to 0, since the rolled materials provide a compressive stress field on the external side. As the materials rotate in such a fluctuating stress field, the region with a high damage value constitutes a ring shaped area.

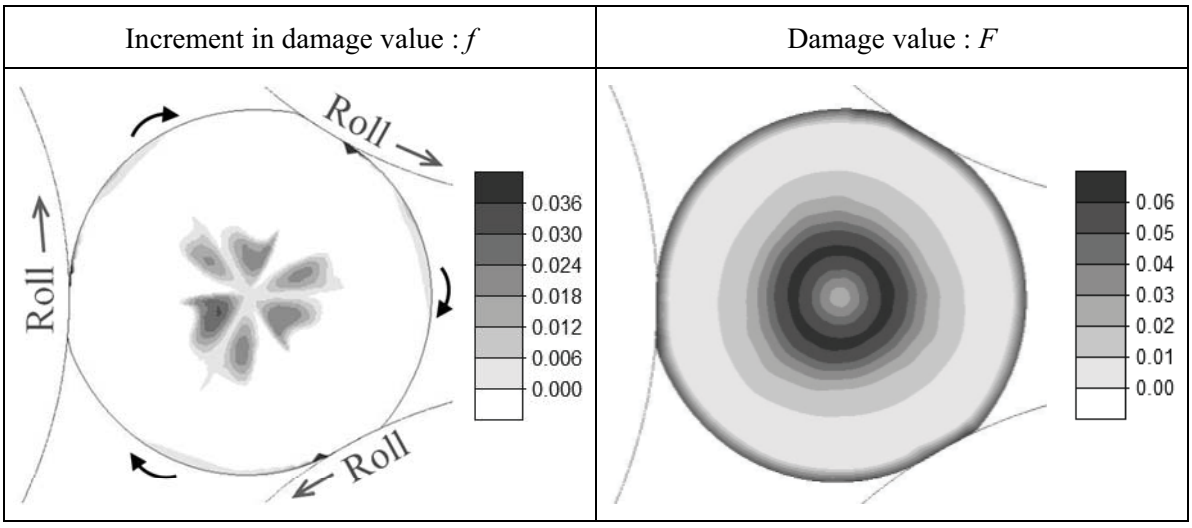

Figure 10: Distribution of damage value using new ductile fracture criterion

Figure 11 shows the contrast between the void density and damage value *F*. The distribution of the void density shown in Fig. 5 qualitatively agrees with that of damage value *F*. In this paper, the number of voids per unit area was measured in such a way as shown in Fig. 2. It is difficult to estimate the void size from the void density since individual voids have their own different volumes. Obtaining quantitative correspondence is a very complicated task; however, we believe that it is necessary to contrast not the void number but the void volume with damage value *F*. It is a future task to clarify the relationship between void growth histories and damage values at arbitrary observation points.

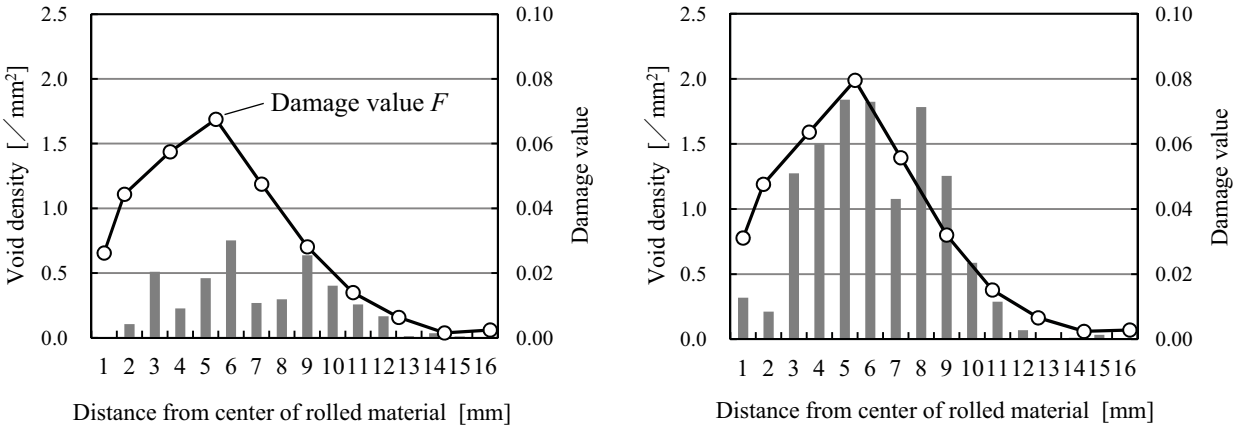

(a) Cross section A (b) Cross section O

Figure 11: Relationship between void density and damage value

5 CONCLUSIONS

- The mechanism of internal fracture in skew rolling has been clarified from hot rolling experiments and numerical analyses. The tensile stress and shear stress that work under plastic deformation induce voids to nucleate, grow and coalesce finally occuring macroscopic internal fracture.
- In three-roll skew rolling, internal fracture occurs around the central axis parts, because a position away from the material's central axis parts constitutes a stress field in which tensile stress and shear stress work simultaneously.
- A new ductile fracture criterion based on tensor quantity, differently from the conventional criteria comprising scalar quantity, has been formulated with tensile stress and shear stress working in the fracture growth direction. This criterion can predict the internal fracture initiation specific to skew rolling. The damage values estimated by this criterion would contribute to the suppression of internal fracture and the optimization of the rolling conditions.
- The proposed ductile fracture criterion is expected to predict internal fracture, regardless of the rolling condition and number of rolls.

REFERENCES

[1] Nakasuji, K., Kuroda, K. & Hayashi, C.: ISIJ Int., **31**-6 (1991), 620-627.
[2] Siebel, E.: Stahl und Eisen, **47** (1927), 1685.
[3] Kocks, F.: Stahl und Eisen, **47** (1927), 433.
[4] New Tube Investments Development: Metallurgia, (1967), 51-56.
[5] Blazynski, T. Z. & Jubb, C.: Journal of the Institute of Metals, **97** (1969), 363-373.
[6] Erman, E.: J. Appl. Metalwork., **4** (1987), 331-341.
[7] Kato, K.: Tetsu-to-Hagané, **56**-7 (1970), 915-929.
[8] Saito, Y., Higashino, T. & Kato, K.: J. Jpn. Soc. Technol. Plast., **17**-191 (1976), 958-965.
[9] Kato, K.: J. Jpn. Inst. Met., **17**-7 (1978), 598-606.
[10] ISIJ: Iron and Steel Handbook 3rd, **2** (1980), 940.
[11] The Japan Society for Technology of Plasticity: Rotary Forming, (1990), 77.
[12] Smirnov, V. S.: Stal', **7** (1947), 511.
[13] Teterin, P. K. & Luzin, Yu. F.: Stal', **10** (1960), 758.
[14] Pater, Zb., Weroñski, W., Kazanecki, J. & Gontarz, A.: J. Mater. Process. Technol., **92-93** (1999), 458-462.
[15] Ayada, M., Higashino, T. & Mori, K.: Adv. Technol. Plast., **1** (1987), 553-558.
[16] Oyane, M.: JSME, **15** (1972), 1507-1513.
[17] Cockcroft, M. G. & Latham, D. J.: Journal of the Institute of Metals, **96** (1968), 33-39.
[18] Rice, J. R. & Tracey, D. M.: J. Mech. Phys. Solids, **17** (1969), 201-217.
[19] McClintock, F. A.: Journal of Applied Mechanics, **35** (1968), 363-371.
[20] Brozzo, P., de Luca, B. & Rendina, R.: International Deep Drawing Research Group, **7** (1972), 3.1-3.5.
[21] Bao, Y. & Wierzbicki, T.: Int. J. Mech. Sci., **46** (2004), 81-98.
[22] Bao, Y. & Wierzbicki, T.: Journal of Engineering Materials and Technology, **126** (2004), 314-324.
[23] Bao, Y. & Wierzbicki, T.: Engineering Fracture Mechanics, **72** (2005), 1049-1069.
[24] Weck, A. & Wilkinson, D.S.: Acta Mater., **56** (2008), 1774-1784.
[25] Li, H., Fu, M. W., Lu, J. & Yang, H.: Int. J. Plast., **27** (2011), 147-180.
[26] Lou, Y., Huh, H., Lim, S. & Pack, K.: Int. J. Solids Struct., **49** (2012), 3605-3615.
[27] Lou, Y. & Huh, H.: Int. J. Solids Struct., **50** (2013), 447-455.